Breaking of time reversal invariance in nonlinear acoustics

Mickaël Tanter,[1]* Jean-Louis Thomas,[1] François Coulouvrat,[2] and Mathias Fink[1]
[1]*Laboratoire Ondes et Acoustique, UMR CNRS 7857, Université Paris VII Denis Diderot, ESPCI, 10 Rue Vauquelin, 75005 Paris, France*
[2]*Laboratoire de Modélisation en Mécanique, CNRS UMR 7607, Université Paris VI, 8 rue du Capitaine Scott, 75015 Paris, France*
(Received 8 December 2000; published 12 June 2001)

Time-reversal invariance of nonlinear acoustic wave propagation is experimentally investigated. Reversibility is studied for propagation shorter or longer than shock formation distance. In the first case, time-reversal invariance holds and a sinusoid distorted by nonlinearities during forward propagation progressively recovers its initial shape after the time-reversal operation. In the second case, reversibility is broken locally at the shock front as a time-reversal operation transforms a stable compression shock into an unstable expansion shock. Achieving experimentally the time-reversal process with a time-reversal mirror made of reversible piezoelectric transducers for very broadband signals, would require transducers with huge bandwidths. To date, such transducers remain unavailable. In order to overcome this technical limitation, we restricted ourselves in this study to one-dimensional (1D) propagation, for which an experimental ersatz of a time-reversal mirror can be used. Indeed, in a 1D case, the time-reversal operation applied on a plane wave can be mimicked for an antisymmetric wave form by a reflection of the plane wave onto a pressure-release interface.

DOI: 10.1103/PhysRevE.64.016602 PACS number(s): 43.35.+d

I. INTRODUCTION

This paper presents experimental results about the reversibility of acoustic wave propagation in the nonlinear regime. In the linear approximation, it is well known that the time-reversal invariance holds for wave propagation in lossless media. Advanced and retarded potential are both solutions of the wave equation. In the low-power regime, time-reversal mirrors made of arrays of reversible piezoelectric transducers are used to switch from one solution to the other [1]. This process is very robust and handles even multiple-scattering medium [2]. For stronger wave amplitudes, nonlinear effects can no longer be ignored. However, ideal-fluid equations remain time-reversal invariant. Hence, for a sinusoidal wave, even if energy is transferred to the harmonic components by nonlinearities during forward propagation, the reversibility ensures that, after time reversal, the signal will recover its initial shape at the fundamental frequency. However, this property holds only as long as the shock formation distance is not reached. For longer propagation, the irreversible loss of energy that occurs at the shock will break the time-reversal invariance. After time reversal, a compression shock will be transformed into an unstable expansion shock, that violates the requirement of entropy increase through the shock and that will evolve as an expansion fan during reverse propagation.

The purpose of this paper is to propose an experimental check of the dependence of time-reversal invariance on the amplitude of the emitted wave. However, carrying out a time-reversal experiment in the nonlinear regime is made a near impossible task by the spreading of energy onto the harmonics. Indeed, the time-reversal operation would require devices with very large bandwidths (several hundred percents), while piezoelectric transducers used in time reversal mirrors have too narrow bandwidths even to transmit back the second harmonic properly. In order to overcome this technical difficulty, we have to restrict ourselves in this paper to a one-dimensional (1D) geometry, for which an experimental ersatz of a time reversal mirror can be used. As explained in the third section, this ersatz is based on the fact that a time-reversal operation for a plane wave is identical to a sign change for an antisymmetric wave form. This last operation can be easily achieved experimentally by a reflection of the plane wave onto a pressure release interface.

In that case, the wave propagation can be described by the inviscid Burgers' equation for an ideal fluid (see Ref. [3] for a review). Thermoviscous absorption can be neglected as the acoustic Reynolds (or Gol'dberg) number $\mathrm{Re}=1/\alpha Ls$, where Ls is the shock distance and α the absorption coefficient, is much greater than one. After a theoretical discussion, we present experimental results and compare them to a numerical simulation of the Burgers equation with a shock capturing numerical algorithm [4].

II. BURGERS' EQUATION AND REVERSIBILITY FOR A PLANE WAVE (THE 1D MODEL)

The nonlinear 1D acoustic equations of mass and momentum conservation write for an ideal fluid:

$$\frac{\partial \rho}{\partial t}+\rho\frac{\partial v}{\partial x}+v\frac{\partial \rho}{\partial x}=0, \tag{1}$$

$$\rho\left(\frac{\partial v}{\partial t}+v\frac{\partial v}{\partial x}\right)+\frac{\partial p}{\partial x}=0, \tag{2}$$

where v, ρ, and p are, respectively, the velocity, the density, and the pressure. For an ideal fluid, entropy remains constant, hence, the equation of state writes:

$$dp=c^2(\rho)d\rho, \tag{3}$$

*Corresponding author. FAX: 33-140-794-468; Email address: michael.tanter@espci.fr

where $c(\rho)$ is the local speed of sound. In these conditions, the exact solution of Euler's equations was found by Riemann in 1860 [3]. He derived a solution by introducing the Riemann invariants:

$$f=\frac{R+\nu}{2}, \tag{4a}$$

$$g=\frac{R-\nu}{2}, \tag{4b}$$

with

$$R(\rho)=\int_{\rho_0}^{\rho} c(\rho)\frac{d\rho}{\rho}, \tag{5}$$

so that Eqs. (1) and (2) can be rewritten as

$$\frac{\partial f}{\partial t}+[c(\rho)+\nu]\frac{\partial f}{\partial x}=0, \tag{6}$$

$$\frac{\partial g}{\partial t}-[c(\rho)-\nu]\frac{\partial g}{\partial x}=0. \tag{7}$$

These two equations describe propagation, respectively, towards $x>0$ with velocity $c+\nu$ and towards $x<0$ with velocity $c-\nu$.

As propagation is nonlinear, these two disturbances interact with one another by modifying the local speed of sound so that Eqs. (6) and (7) are coupled. However, if there is initially no wave propagating towards $x<0$ $[g(x,0)=0]$, it remains so all the time; hence, $R=\nu$ and $f=\nu$.

Expanding the speed of sound up to order 1 in the Mach number, $M=\nu/c$, and using the impedance relation between velocity and acoustical density fluctuations $\nu=\pm dp/\rho_0 c_0$ (+ for forward propagation, − for backward propagation) yields

$$c(\rho)=c_0+\frac{B}{2A}\nu+o(M), \tag{8}$$

where B/A is the nonlinearity parameter [3] ($\cong 5$ in water) and c_0 the speed of sound at equilibrium. The magnitude of the acoustic perturbation is measured by the Mach number that remains very small, less than 10^{-3} in our water experiment and in most situations, ensuring the validity of this approximation.

Introducing Eq. (8), Eq. (6) becomes:

$$\frac{\partial \nu}{\partial t}+(c_0+\beta\nu)\frac{\partial \nu}{\partial x}=0, \tag{9}$$

where $\beta=B/2A+1$. Similarly, considering only waves propagation towards $x<0$, yields:

$$-\frac{\partial \nu}{\partial t}+(c_0-\beta\nu)\frac{\partial \nu}{\partial x}=0\,. \tag{10}$$

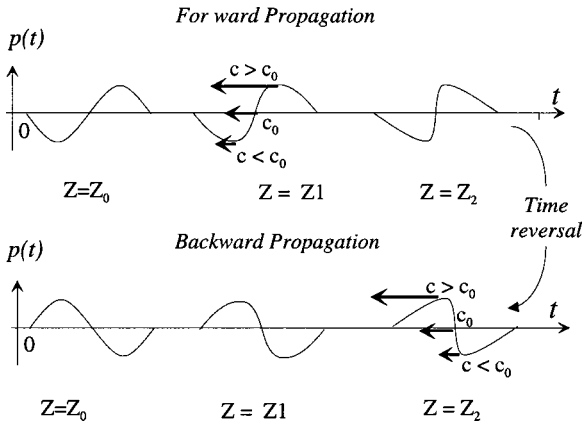

FIG. 1. A time-reversal experiment for a one-dimensional nonlinear propagation. The signal $p(t)$ received at position $x=x_0$ is time reversed $[p(T-t)]$ and reemitted towards $x<0$.

In a frame of coordinates moving with velocity c_0, these two equations can be transformed into the inviscid Burgers' equation.

Equations (9) and (10) generalize to nonlinear acoustics the factorization of the second-order linear wave equation into two first-order one-way equations. The main difference is that, in nonlinear acoustics, the actual sound velocity $c_0 \pm \beta\nu$ depends on the instantaneous value of the acoustic field. The different parts of the wave form propagate at slightly different velocities, thus leading to the distortion of the wave profile with a steepening of ascending parts of the wave profile and a flattening of descending ones. This process results in discontinuity or shock formation at a distance equal (for a sinusoidal wave) to

$$L_s=\frac{1}{k\beta M}, \tag{11}$$

where k is the wave number.

For propagation distances longer than L_s, Burgers' equation is insufficient to determine the position of shocks and must be complemented by the so-called ''equal area rule,'' which is the low-amplitude approximation of Rankine-Hugoniot relations for shock waves. This point will be addressed later. In this first section, let us examine time-reversal invariance of nonlinear wave propagation before reaching the shock distance.

A time-reversal operation in a one-dimensional configuration is described in Fig. 1. The forward propagation is described by Eq. (9), $\nu(x,t)$ is measured at some position $x=x_0$ smaller than the shock distance, and its time dependence is recorded. After some delay T ensuring causality, the record is played backward generating a wave propagating towards $x<0$. The evolution of this time-reversed wave is now described by Eq. (10) with the new boundary condition at x_0: $g(t)=-\nu(T-t)$. It is immediate to check that, if $\nu(x,t)$ is a solution of Eq. (9) then $-\nu(x,T-t)$ is a solution of Eq. (10). Hence, the time-reversal invariance holds even in a nonlinear regime. The change of sign comes from the fact that $\nu(t)$ is a first-order time derivative of the displacement (a ''flux'' quantity in thermodynamics terms). In prac-

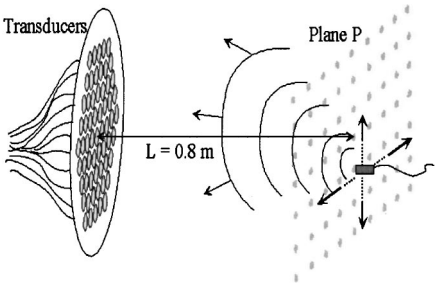

FIG. 2. A pointlike source scans the plane *P*, generating for each location a diverging spherical wave that is received and stored on each transducer of the array. This procedure simulates a digitized plane source of equivalent aperture.

tice, pressure is more usually recorded than velocity. The impedance relation between p and v, which are in phase for forward propagation and antiphase for backward propagation, implies that, on the contrary, during a time-reversal experiment, $p(t)$ is transformed in $p(T-t)$ (pressure is an ''affinity'' quantity in thermodynamics terms).

Time-reversal invariance is illustrated by Fig. 1: during forward propagation, overpressures propagate faster than underpressures and the signal distorts. After a time-reversal operation, overpressures are now back emitted in late compared to underpressures, a delay that will be progressively made up during backward propagation by their highest velocity. The signal will progressively undistort and finally recover its initial sinusoidal shape.

III. EXPERIMENTAL SETUP

To realize this scheme experimentally, the first step consists in synthesizing a wave as plane as possible along the mirror aperture. This is achieved by working in the near field of a plane piston. Thus, the wave remains collimated and diffraction effects are reduced. This piston is made up of an array of 61 transducers working at a central frequency of 1 MHz and immersed in water. Transducers—8 mm diameter disks—are set up with a 10 mm step on an hexagonal pattern (Fig. 2). This arrangement gives a total aperture $D=0.09$ m resulting in a Fresnel distance of $D^2 4\lambda = 1.2$ m. Each transducer is wired to an electronic channel with its own programmable transmitter, an 8-bits dynamics and a 30-MHz sampling rate, providing complete control of the amplitude and time dependence of the signals.

A plane wave is synthesized by scanning a control plane (in practice, the plane of time reversal) with a point source at numerous positions, collecting on each transducer of the emitting array the corresponding responses (Fig. 2). Summing the contributions from all source positions, a set of 61 signals is computed (Fig. 3). This step of the procedure is linear as the point source is very weak. Time reversing these 61 signals and using them to drive the transducers generates an almost plane wave front in the control plane, as controlled experimentally on the phase (Fig. 4). This procedure minimizes diffraction effects, for instance, the amplitude distribution of the sources in the control plane is apodized in order to decrease edge waves effects. In this configuration, a plane

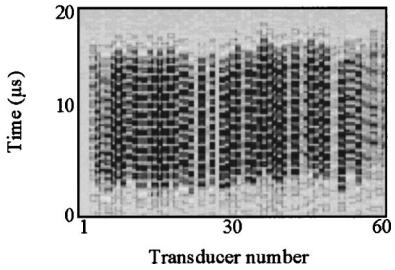

FIG. 3. Computed signal received onto the array when the digitized plane source transmits a wave packet.

wave with an amplitude up to 5 Atm can be generated. For such a wave, the shock distance is 0.3 m.

The second step consists of achieving a time reversal of the synthesized plane wave. Unfortunately, achieving experimentally a time-reversal operation by the use of an another time-reversal mirror (TRM) would require devices with very large bandwidths (to re-emit the harmonics resulting from signal distortion during forward propagation), while piezoelectric transducers used in our TRMs have too narrow bandwidths even to transmit back the second harmonic properly. To overcome this problem, the proposed trick is to remark that, for 1D problems and for an antisymmetric wave packet $[p(-t)=-p(t)]$, a time reversal $[p(-t)]$ is identical to a reflection onto a pressure release interface $[-p(t)]$ (Fig. 5). This trick is valid in the nonlinear regime because nonlinear propagation keeps the antisymmetry of a signal. Nonetheless, this trick does not allow us to re-emit the time-reversed signal with a time-delay T, so that incident and reflected waves will interact close to the interface. However, it is well known that nonlinear interaction between counterpropagating acoustic waves are not cumulative. Hence, they remain very small compared to the large distortions obtained by the self interaction of one-way waves.

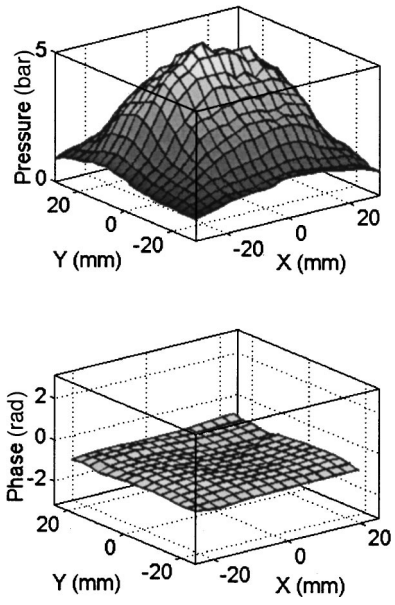

FIG. 4. Spatial distribution of amplitude and phase in plane *P* of the wave front generated by transmitting signals of Fig. 3 after time reversal.

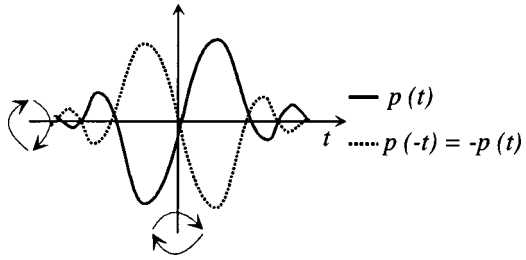

FIG. 5. The time-reversed version of an antisymmetric time signal is equivalent to its opposite: The time-reversal operation can be mimicked by a reflection onto a water-air interface (reflection coefficient $r=-1$).

To obtain pressure-release reflection, a 13-μm Mylar sheet is stretched on a hollow cylindrical shell in order to make a water-air interface. A thin sheet is required to avoid any filtering even for the higher harmonics. The interface is set in the plane $z=0.8$ m away from the array (Fig. 6).

IV. REVERSIBILITY OF A SIMPLE WAVE

First of all, reversibility is checked in the case of a shock distance of 1.1 m (1.7 Atm wave amplitude), larger than the propagation distance array-Mylar sheet. Figure 7 presents measurements of the pressure wave forms at two locations along the axis z: $z=-0.4$ m (solid line) and $z=-0.02$ m (dashed line). Distances are measured from the water-air interface and are noted negative/positive for forward/backward propagation. One can observe the nonlinear steepening of the profile during forward propagation. The experimental signals are compared to a numerical simulation of the inviscid 1D Burgers equation. This simulation is achieved by the use of the hybrid finite differences scheme of MacDonald and Ambrosiano [4]. It combines a second-order finite differences scheme when the signal is smooth with a one-sided, first-order scheme that prevents artificial dispersive ripples to appear near sharp gradients while ensuring monotonicity. Clearly, the Burgers equation reproduces the measured distortion of the wave profiles as the signal propagates further.

Time-reversal invariance means that, at each position, the time wave forms during forward and backward propagation are the time reversal of one another. We check this property experimentally for two depths: at mid distance, $z=\pm 0.4$ m

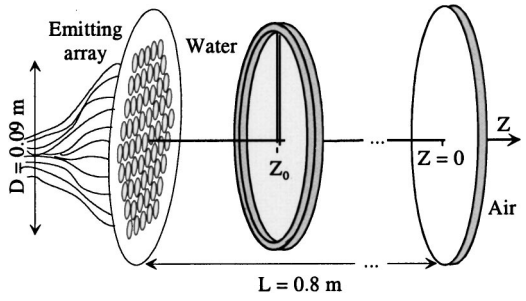

FIG. 6. Experimental setup. A transducer array radiates a quasiplane wave. A bilaminar hydrophone records the signal received at location z_0. The plane wave is reflected on a plane water-air interface and back propagates towards the initially emitting array.

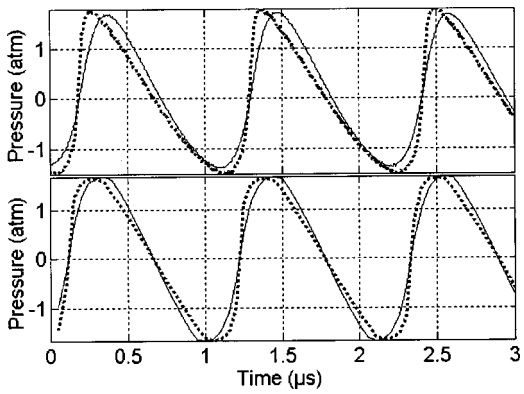

FIG. 7. Time dependence of the pressure in atmosphere for a zoom of the wave packet at mid distance, $z=-0.4$ m solid line, and close to the pressure release interface, $z=-0.02$ m dashed line. Top figure, experiment; bottom figure, the one-dimensional numerical simulation of the Burgers equation.

(Fig. 8) and close to the emitting array, $z=\pm 0.8$ m (Fig. 9). Both figures compare the measured signals during the forward (solid line) and backward propagation (dashed line). For this comparison, backward signals have been changed in their opposite (as signals here are antisymmetric). It clearly appears on the figure that the forward and backward signals at both locations almost perfectly superpose: time-reversal invariance is satisfied, the nonlinear distortion of the wave profile has been balanced by time reversal. It is especially spectacular near the emitting array, where the backward signal has perfectly recovered its initial sinusoidal shape. The transfer of energy from the fundamental to the harmonics during forward propagation has been completely reversed during backward propagation. The phenomenon of nonlinear distortion healing by a pressure-release interface was observed previously [5] and has been used to delay nonlinear attenuation [6] but, to our knowledge, has never been linked to the time-reversal invariance.

It is to be noted that, to get a perfect superposition of

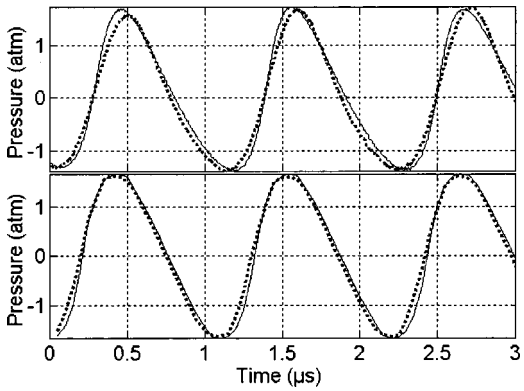

FIG. 8. Comparison of pressure dependence at mid distance ($z=-0.4$ m solid line, and $z=+0.4$ m dashed line). Signals corresponding to backward propagation have been multiplied by -1 in order to allow exact comparison. Top figure, experimental results; bottom figure, numerical results. In experimental results, the dashed curve has been multiplied by 1.15 to compensate for diffraction spreading.

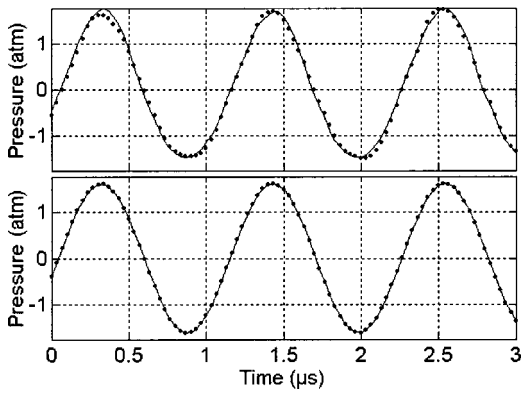

FIG. 9. Comparison of pressure dependence at the beginning of the forward propagation ($z=-0.8$ m solid line), and at the end of the backward propagation ($z=+0.8$ m dashed line). Signals corresponding to backward propagation have been multiplied by -1 in order to allow exact comparison. Top figure, experimental results; bottom figure, numerical results. In the experimental results, the dashed curve has been multiplied by 1.75 to compensate for diffraction spreading.

forward and backward signals, the amplitudes of these last ones had to be enhanced to compensate for diffraction spreading. However, this compensation factor has been checked experimentally to fit the amplitude decrease due to linear diffraction acoustics when the emitted signal is much weaker. Therefore, it is related only to pure, linear diffraction. This means that, though our experiment is not perfectly 1D due to the finite size of the emitter, our time-reversal ersatz is very robust and ensures an almost perfect time reversal, independently of any diffraction effect.

V. IRREVERSIBILITY OF A SHOCK WAVE

For a propagation distance longer than L_s, the overpressures that propagate faster overtake the underpressures, leading to an unphysical multivalued wave profile. To recover a physically acceptable solution, a discontinuity, or shock wave, must be introduced that skips the multivalued part of the profile. The position of this shock is determined according to Rankine-Hugoniot relations [3,7], that express the principles of mass, momentum, and energy conservation through the shock. Also, Rankine-Hugoniot relations state that, according to the second principle of thermodynamics, the entropy must increase through the shock:

$$s_2 - s_1 \geqslant 0. \tag{12}$$

Therefore, even in an ideal fluid, shock formation is an irreversible process that breaks the time-reversal invariance. For small amplitude acoustic waves, Rankine-Hugoniot relations can be approximated by the ''equal area rule,'' according to which the two lobes of the multivalued solution skipped by the shock must be of equal areas. Entropy inequality also implies that only compression shocks are thermodynamically acceptable (for fluids such that $\beta \geqslant 0$).

Of course, an abrupt shock is only a mathematical idealization of physical reality. Shock waves correspond to regions of sharp gradients where thermoviscous dissipation cannot be neglected anymore. The two parts of the wave profile on each side of the shock are indeed connected by a very rapid but continuous transition. This tiny shock structure realizes a dynamical balance between dissipative smoothening and nonlinear steepening. For thermoviscous absorption, this shock structure is described by the Taylor's shock structure [8] (a hyperbolic tangent). However, the position of the shock and the energy loss through it, can be described independently of the physical mechanism of energy absorption (provided this last one is small enough). This explains why numerical simulations (that introduce artificial numerical dissipation to stabilize solutions at the discontinuity) or experimental measurements (that introduce additional attenuation due to the hydrophone filtering of high frequencies) nevertheless reproduce the shock positions and amplitude.

Time reversing a compression shock leads to an expansion shock that violates the second principle and will therefore be unstable. Solving the inviscid Burgers equation with an initial expansion shock, the method of characteristics shows two diverging characteristics emanating from each side of the shock (because the overpressure part already ahead propagates faster) and leaving a ''blank'' in between. This blank is filled up by a centered expansion fan of characteristics, so that the two diverging parts of the initial discontinuity are connected by a straight line [9]. This situation is analogous to the centered Prandtl-Meyer fan for a supersonic flow around a sharp corner. Therefore, for an initially sinusoidal wave propagating longer than the shock distance, the ''signature'' of the breaking of time-reversal invariance by irreversible shocks will be, after backward propagation, this expansion fan that will persist and never coincide with any part of the initial signal. If taking into account dissipation, this instability can be explained in other words by the fact that now dissipation and nonlinear distortion act concurrently for an expansion shock, instead of counterbalancing for a compression shock.

To check the breaking of time-reversal invariance, the same experiment as described previously is reproduced, but now the emitted amplitude is 5 Atm, resulting in a shock distance of 0.3 m smaller than the propagation distance. The steepening is now much faster, and sharp shocks are formed when the wave impinges on the water-air interface (Fig. 10, compare to Fig. 7). The signal at mid distance (solid line) is shocked but descending parts keep some sinusoidal shape whereas, at the end of forward propagation (dashed line), a shape close to a sawtooth profile is obtained.

The numerical simulations show a good agreement compared to the experimental signals. The little differences between simulation and experiment are only due to diffraction effects that are of course not taken into account in the 1D numerical scheme, and which are known to produce the slight asymmetry of the signal with enhanced peaks.

Breaking of time-reversal invariance is illustrated by Figs. 11 and 12 where forward and backward time wave forms are compared at the same location at mid distance, $z=\pm 0.4$ m (Fig. 11) and near the emitting array, $z=\pm 0.8$ m (Fig. 12). The *same* correction factors as for the previous case have been used to compensate for diffraction spreading. Compared to the moderate amplitude case for which shock dis-

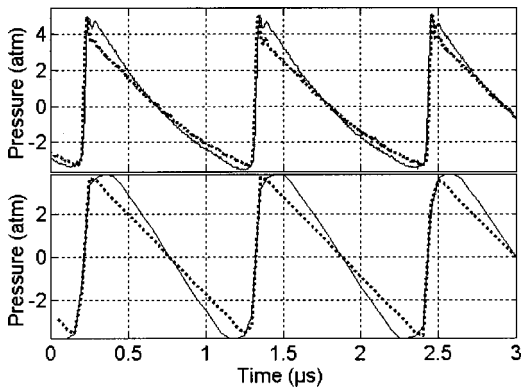

FIG. 10. Time dependence of the pressure in atmosphere at mid distance, $z=-0.4$ m solid line, and close to the pressure release interface, $z=-0.02$ m dashed line. Top figure, experiment; bottom figure, numerical simulation.

tance was not reached and superposition was almost perfect (Figs. 8 and 9), the profiles are now far from superposing one another. It is clear in Fig. 11 that the forward shock waves have been time reversed into backward expansion fans that do not superpose at all (neither in amplitude or slope), a proof that the breaking of time-reversal invariance is due to the reversal of stable compression shocks into unstable expansion shocks. On the contrary, the other parts of the wave profile that have not sustained irreversible losses perfectly superpose on numerical simulations. This superposition is not so perfect on experimental measurements due to the diffraction asymmetry of the profiles (positive overpressure on the descending part), but remains obvious on a significant part of the wave forms.

The same conclusions can be drawn from Fig. 12 (compared to Fig. 9) at the end of the process. Once again, the straight line resulting to the time reversal of the shock waves do not superpose to the ascending parts of the incident signal that lead to shock formation, while the descending parts of

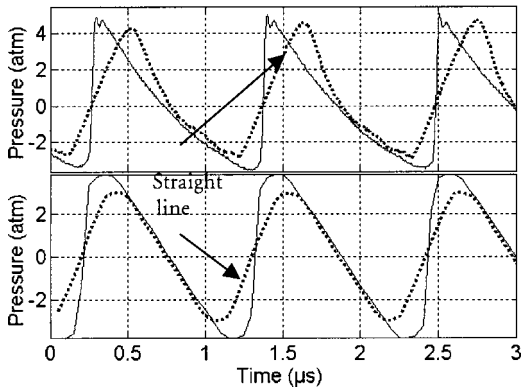

FIG. 11. Comparison of pressure dependence at mid distance ($z=-0.4$ m solid line, and $z=+0.4$ m dashed line) during forward and backward propagation. Signals corresponding to backward propagation have been multiplied by -1 in order to allow exact comparison. Top figure, experimental results; bottom figure, numerical results. In experimental results, the dashed curve has been multiplied by 1.15 to compensate for diffraction spreading.

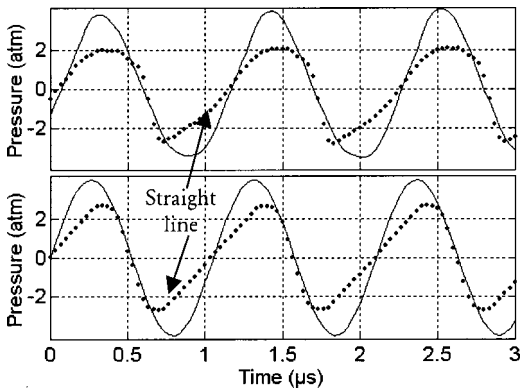

FIG. 12. Comparison of pressure dependence at the beginning of forward propagation and at the end of backward propagation ($z=-0.8$ m solid line, and $z=+0.8$ m dashed line). Signals corresponding to backward propagation have been multiplied by -1 in order to allow exact comparison. Top figure, experimental results; bottom figure, numerical results. In the experimental results, the dashed curve has again been multiplied by the 1.75 factor compensating for linear diffraction spreading.

the wave profiles that have not undergone irreversible shocks recover almost perfectly their initial shape, both for experimental and numerical simulations.

VI. CONCLUSION

A time-reversal experiment has been carried out in nonlinear acoustics. To overcome the impossibility of realizing a time-reversal mirror with a sufficient band-width, an ersatz has been used at one dimension by noting that, for antisymmetric wave forms, time reversal is equivalent to reflection onto a pressure-release interface. This experiment has been conducted in a weakly viscous medium for which classic linear attenuation is negligible at the fundamental frequency. Up to the shock formation, the reversibility holds and the energy stored in the harmonics components returns to the fundamental after the time reversal. Hence, a simple wave distorts as it travels towards the reflector and undistorts thereafter. The perfect superposition of incident and reflected wave profiles has been checked experimentally. On the contrary, the wave undergoes an irreversible alteration when a shock is formed, always implying dissipation and thus breaking the time-reversal invariance. Time reversal changes shocks into expansion shocks that are unstable because dissipation and nonlinearity work together to smooth it. During backpropagation, the part of the signal corresponding to this inverted shock remains as a straight line whose slope decreases rapidly, so that the initial wave form cannot be recovered. On the contrary, other parts of the signal that have not undergone irreversible shocks recover their initial shape, as proved experimentally. This last point emphasizes that the breaking of time-reversal invariance in nonlinear acoustics is identified to the energy loss through shocks and to their reversal as unstable expansion shocks.

[1] M. Fink, Phys. Today **50**, 34 (1997).
[2] A. Derode and M. Fink, Phys. Rev. Lett. **75**, 4206 (1995).
[3] M. F. Hamilton and D. T. Blackstock, *Nonlinear Acoustics* (Academic, New York, 1998).
[4] B. E. McDonald and J. Ambrosiano, J. Comput. Phys. **56**, 448 (1984).
[5] A. L. VanBuren and M. A. Breazeale, J. Acoust. Soc. Am. **44**, 1014 (1968).
[6] T. G. Muir, L. L. Mellenbruch, and J. C. Lockwood, J. Acoust. Soc. Am. **62**, 271 (1977).
[7] L. Landau and E. Lifchitz, *Fluids Mechanics* (Mir Editions, Moscow, 1971), Vol. 6, Chap. 9, p. 85.
[8] G. I. Taylor, Proc. R. Soc. London, Ser. A **84**, 371 (1910).
[9] G. B. Whitham, *Linear and Nonlinear Waves* (Wiley, New York, 1974), pp. 24, 204.